31 Supplementary Methods

32 Ovalbumin (OVA)-driven CD4⁺ T cell cultures and intracellular cytokine staining

- 33 Mesenteric lymph nodes cells from reconstituted and OVA-sensitized GF mice were
- 34 labeled with the Violet CellTrace proliferative dye (Invitrogen; Grand Island, NY) and
- 35 cultured with 200µg/ml OVA and 250pg/ml IL-2 for 72 hours. During the last 4 hours,
- 36 cultured cells were stimulated with PdBU (500 ng/ml; Sigma-Aldrich, St. Louis MO) and
- 37 Ionomycin (500 ng/ml; Sigma-Aldrich) in the presence of Brefeldin A (1µg/ml; BD
- 38 Biosciences San Jose, CA). Cells were stained with the following conjugated
- antibodies: CD3 (145-2C11), CD4 (RM4-5), IL-4 (11B11) and IFN-γ (XMG1.2)
 (eBioscience, San Diego, CA). Intracellular cytokines were detected in Violet CellTrace⁺
 proliferating CD3⁺CD4⁺ T cells by using Cytofix/Cytoperm (BD Biosciences) buffers,
- 42 according to the manufacturer's instructions. Stained cells were analyzed on a LSRII
- 43 Fortessa cytometer (BD Biosciences) and data processed using Flowjo (Tree Star;

44 Ashland, OR).

45 **PhyloChip[™] data analysis**

Pre-processing and Data Reduction. Fluorescent images were captured with the 46 47 GeneChip Scanner 3000 7G (Affymetrix, Santa Clara, CA). An individual array feature 48 occupied approximately 8x8 pixels in the image file corresponding to a single probe 49 25mer on the surface. To calculate the summary intensity for each feature on each 50 array, the central 9 pixels of individual features were ranked by intensity and the 75% 51 percentile was used. Probe intensities were background-subtracted and scaled to the 52 PhyloChip[™] Control Mix. Array fluorescence intensity was collected as integer values ranging from 0 to 65,536 (2¹⁶). Fluorescence intensities for sets of probes 53

54 complementing an operational taxonomic unit (OUT) were averaged after discarding the 55 highest and lowest and the mean was log₂ transformed into numbers ranging from 0 to 56 16. For compatibility with some statistical operations, the scores were multiplied by 57 1000 then rounded, allowing a range of integers from 0 to 16,000. These values are 58 referred to as the hybridization score (HybScore). For the complete distribution see Hazen et al, Supplemental Information¹. The data was reduced to consider the 59 bacterial taxa deemed present as described in Hazen et al.¹. Taxa were filtered to 60 61 those present in the majority of samples of at least one of the experimental groups and 62 rank-normalized such that taxa in each are represented by their ranked HybScore within 63 that sample only (rank 1 represents the lowest HybScore in that sample).

64 Sample-to-Sample Distance Function. All profiles were inter-compared in a pair-wise fashion to determine a dissimilarity score and results were stored as a distance matrix. 65 66 The Weighted Unifrac distance measure was chosen because it utilizes the 67 phylogenetic distance between OTUs as well as the abundance of those OTUs to compute a community-wide dissimilarity between any pair of profiles ^{2, 3}. Similar 68 69 biological samples produce small Weighted Unifrac dissimilarity scores. When 70 comparing the presence or absence of taxa between profiles, the Unweighted Unifrac 71 distance measure was utilized.

Statistical Analysis, Ordination, Clustering, and Classification Methods. The differences between the microbial communities (the entire number of OTUs detected in any one comparison group versus another) was determined by the Adonis test, which is a permutation test based on a dissimilarity matrix, in this case measured by weighted UniFrac. Because the Adonis test considers the multidimensional structure of the data (e.g., compares entire microbial communities), it does not involve multiple hypotheses
 testing for each microbial taxon found within those communities.

79 Taxa found increased in their ranked HybScore in one category compared to the 80 alternate categories were identified using the Kruskal-Wallis (KW) test. The aim of a KW 81 filter in the context of this analysis was to reduce the dimensionality of the dataset, and 82 demonstrate that this reduced set of OTUs could still effectively discriminate between 83 samples in terms of their microbial community structures by the ordination and 84 clustering methods listed below.

85 Two-dimensional ordinations and hierarchical clustering maps of the samples in the form of dendrograms were created to graphically summarize the inter-sample 86 relationships. To create dendrograms, the samples from the distance matrix are 87 clustered hierarchically using the average-neighbor (HC-AN) method ⁴. Non-Metric 88 89 Multidimensional Scaling (NMDS) was employed to visualize relationships between samples by two-dimensional ordination plotting ⁵. Ordination points are colored by 90 91 highlighted groupings. Lists of significant taxa whose abundance characterizes each 92 class is performed using Prediction Analysis for Microarrays (PAM), a classifier 93 (supervised machine learning) based method that utilizes a nearest shrunken centroid method ⁶. 94

95 *Phylogenetic Tree Visualization.* Bacterial families with OTUs found by the KW test to 96 be differentially abundant between two comparison groups (*e.g.* allergen sensitized WT 97 versus *Il4raF709* mice) were identified, and the one OTU with the greatest difference 98 between the two group means from each family was selected. For those families 99 containing OTUs with both higher and lower abundance scores between the two comparison groups, two OTUs were selected. A phylogenetic tree was constructed
 using FastTree, which was built using one representative 16S ribosomal DNA (rDNA)
 gene sequence from each of the OTUs selected from the Greengenes multiple
 sequence alignment ^{7, 8}. The Tree was displayed with iTOL software ⁹.

104 16S rDNA sequencing methods and data analysis

105 Summary of methodology. The microbial community structure in each stool sample was 106 assessed by 16S amplicon sequencing on the Roche 454 platform. Sequencing data 107 was processed through a bioinformatics pipeline to obtain distributions of OTUs for each 108 sample. We tested differences in overall microbial community structure between stool 109 samples from different groups using the Dirichlet Multinomial model and a likelihood ratio test ^{10, 11}. We used hierarchical clustering with the Bray-Curtis (BC) dissimilarity 110 111 measure to visualize the differences between the distributions of OTUs in samples ¹². 112 The BC measure quantifies the difference between a pair of ecosystems based on the 113 species or OTU composition of samples. A BC value of zero indicates identical OTU 114 distributions; a BC value of one indicates no overlap in the OTUs present in the pair of 115 samples. We used a bootstrapping procedure to estimate 95% confidence intervals on 116 BC measures, and thus evaluate the reproducibility of sample clusterings. Results were 117 visualized with a dendrogram constructed using the bootstrapped values. We also used 118 the UniFrac measure with Principal Coordinates Analysis (PCoA) to visualize 119 differences between microbial communities in samples; this measure takes into account 120 phylogenetic relationships among sequences and does not require clustering sequences into OTUs ^{2, 3}. Individual OTUs that discriminate between different groups 121 were determined using a Random Forests supervised machine learning approach ^{13, 14}. 122

123	16S rDNA Amplicon sequencing. DNA pyrosequencing was performed by the Human
124	Genome Sequencing Center at Baylor College of Medicine following protocols
125	benchmarked for the Human Microbiome Project. The V3-V5 hypervariable regions of
126	the 16S rRNA gene were amplified using primer 357F (5'-CCTACGGGAGGCAGCAG-
127	3') modified with the addition of the 454 FLX-titanium adaptor "B" sequence
128	(5'CCTATCCCCTGTGTGCCTTGGCAGTCTCAG-3') and primer 926R (5'-
129	CCGTCAATTCMTTTRAGT-3') modified with the addition of unique 6-8 nucleotide
130	barcode sequences and the 454 FLX-titanium adaptor "A" sequence (5'-
131	CCATCTCATCCCTGCGTGTCTCCGACTCAG-3'). Barcode and adaptor sequences
132	are found at
133	http://www.hmpdacc.org/doc/HMP_MDG_454_16S_Protocol_V4_2_102109.pdf. PCR
134	amplification was performed on 2 uL of DNA template in a total volume of 25 uL
135	containing 1x AccuPrime Buffer II (Invitrogen Corp., Carlsbad, CA), 320 uM of each
136	primer, and 0.03 U/uL AccuPrime High Fidelity Taq polymerase. Reactions were
137	heated at 95°C for 2 min followed by 30 cycles of 95°C for 20 sec, 50°C for 30 sec, and
138	72°C for 5 min. The concentration of amplicons in each reaction was determined in
139	triplicate using the PicoGreen fluorescent assay (Invitrogen Corp.) and amplicons were
140	pooled before being sequenced via a multiplexed 454-FLX-titanium pyrosequencing run
141	according to manufacturer's specifications.
142	Bioinformatics for 16S data. Sequences were pre-processed using custom scripts and
143	the packages mothur, CloVR, and QIIME ¹⁵⁻¹⁷ . Filtering criteria were: no ambiguous
144	bases, maximum homopolymer length of 8, 1 base difference allowed for barcode
145	matches, and 2 base differences allowed for primer matches. Each sample had

146	approximately 3000 reads after filtering. Sequences were trimmed based on a minimum
147	average quality score of 35 over a window of length 50 nt, and clustered into OTUs with
148	a similarity threshold of 95%.

- 149 <u>Testing for differences in OTU distributions between groups. OTU relative abundances</u>
- 150 were assumed to follow the Dirichlet Multinomial (DM) distribution^{1,2}. To test for
- differences in overall community structure between two groups, denoted A and B, we
 used a likelihood ratio test:
- 153 $S = -2\ln\{P(X_A, X_B | M_{A+B}) / [P(X_A | M_A) P(X_B | M_B)]\}$
- 154 Here, X_A and X_B represent the set of vectors of OTU counts for groups A and B

155 respectively. M_{A+B} represents the DM model estimated from the combined groups, and

156 <u>M_A and M_B the corresponding DM models estimated from the separate groups. DM</u>

157 parameters were estimated using the Maximum Likelihood method. The S statistic

158 asymptotically follows a χ^2 distribution with degrees of freedom equal to the number of

159 OTUs in the samples.

160 Clustering and visualizing samples. Bootstrapping was performed to standardize the 161 effects of differing numbers of sequencing reads between samples, and to obtain 162 estimates of the variability of dissimilarity measures between samples. For each pair of 163 samples i and j, m reads were drawn independently and with replacement, and the Bray-Curtis Dissimilarity measure³ was calculated between the bootstrapped reads. We 164 165 set *m* equal to the median number of sequencing reads over all samples, and repeated 166 the bootstrapping procedure on each pair of samples 10,000 times. The 95% confidence interval for each sample pair was then estimated from the empirical 167

168 <u>distribution of values. An average linkage dendrogram was constructed using the 95th</u>
 169 <u>centile values between nodes.</u>

170 <u>Finding OTUs that discriminate between groups.</u> To find OTUs discriminating between 171 groups, we used Random Forests⁵ (RF) with a wrapper feature based method as 172 implemented in the Boruta⁶ package. Briefly, RF is an ensemble based classification 173 method that uses multiple weak classifier decision trees. An importance measure is 174 calculated for each feature (OTU) based on the loss of accuracy in classification. The 175 statistical significance of the importance measure is determined using a permutation 176 based method.

177 16S rDNA Pyrosequencing Analysis: Results

178 Comparisons between sensitized and sham sensitized II4raF709 mice. We assessed 179 the difference in overall microbial community structure among stool samples from 180 Il4raF709 homozygous mutant mice sensitized with OVA or sham sensitized with PBS. 181 The distributions of OTUs differed significantly between the groups (Dirichlet Multinomial model, p-value = $< 10^{-20}$). BC dissimilarity dendrograms and UniFrac PCoA 182 183 plots visualizing differences in overall microbial community structure between groups 184 showed overall separation between the two groups, although two mutant PBS samples 185 were close to outlying mutant OVA samples (Figure E1A, B). Several bacterial families 186 and genera were found to discriminate between the groups using a supervised machine 187 learning based method, including OTUs classifying to the genera Clostridium, 188 Bacteroides, Alistipes and Streptococcus (Table E3).

189 <u>Comparisons between unsensitized WT versus II4raF709 mutant mice. We assessed</u>

190 the difference in overall microbial community structure between stool samples from

191 unsensitized WT and *Il4raF709* homozygous mutant littermate mice, and found that the 192 distributions of OTUs differed significantly between the two groups (Dirichlet Multinomial model *P* value = 7×10^{-11}). We visualized differences in overall microbial community 193 194 structure between the two groups using a dendrogram with the BC measure (Figure E4A) and a UniFrac PCoA plot (Figure E4B). Consistent across both techniques, the 195 196 samples from the II4raF709 homozygous mutant mice overall clustered together, 197 although few WT samples clustered with outlying *II4raF709* samples. These findings 198 suggest that differences between the two groups were relatively subtle and not well-199 visualized using a dimensionality reduction method. To explore differences in individual 200 OTUs, we used a supervised machine learning based method, and found differences in 201 several OTUs, including those classifying to the genera Helicobacter, Clostridium, 202 Lactobacillus and Odoribacter (data not shown). 203 Comparisons between WT and II4raF709 mutant sensitized mice. We assessed the 204 difference in overall microbial community structure among stool samples from *Il4raF709* 205 homozygous mutant mice and WT controls sensitized with OVA. The distributions of 206 OTUs differed significantly between each group (Dirichlet Multinomial model, P value = < 10⁻²⁰). BC dissimilarity dendrograms and UniFrac PCoA plots visualizing differences in 207

- 208 overall microbial community structure between groups showed clear separation
- 209 between the WT and mutant OVA groups (Figure E5A, B). Several bacterial families
- 210 and genera were found to optimally discriminate between the groups using a supervised
- 211 machine learning-based method, including Alistipes, Clostridium, Anaeroplasma,
- 212 Lachnobacterium, and Bacteroides (Table E9).

213 Assessing recolonization of WT GF mice by flora of OVA-sensitized WT versus mutant 214 mice. We assessed the difference in overall microbial community structure between 215 stool samples from the two groups of recipient mice collected 8 weeks after colonization 216 (at the end of the OVA sensitization period). The distributions of OTUs in stool samples 217 from the group of mice receiving donor microbiota from allergen-sensitized mutant mice 218 differed significantly from those of the group receiving donor microbiota from WT mice (Dirichlet Multinomial model^{1,2} P value < 10⁻²⁰). We visualized differences between 219 220 samples using a dendrogram with the BC measure (Figure 8A). 221 The samples from the group of mice that received donor microbiota from WT mice all 222 clustered tightly, and clustered with the respective donor sample. The samples from the 223 group of mice that received donor microbiota from allergen-sensitized *II4raF709* mutant 224 mice also clustered closely with one another, but were distinct from those of WT flora 225 recipients. The donor sample from allergen-sensitized mutant mice essentially clustered

- 226 <u>separately, but was closer to its respective recipient samples in aggregate than it was to</u>
 227 <u>the other samples.</u>
- 228 Supplementary Figure Legends
- Figure E1. The microbial signature and dysbiosis associated with the allergen sensitization of *II4raF709* mice is reproduced by 16S rDNA pyrosequencing. A. Agglomerative clustering of fecal samples from OVA- and sham PBS sensitized *II4raF709* mice based on 16S OTUs Samples were clustered based on bootstrapped BC dissimilarity values computed on the relative abundances of OTUs in each sample.
 BC = 0 indicates identical microbial communities; BC = 1 indicates communities with no overlapping OTUs. Heights of lines on the dendrogram indicate bootstrapped BC values

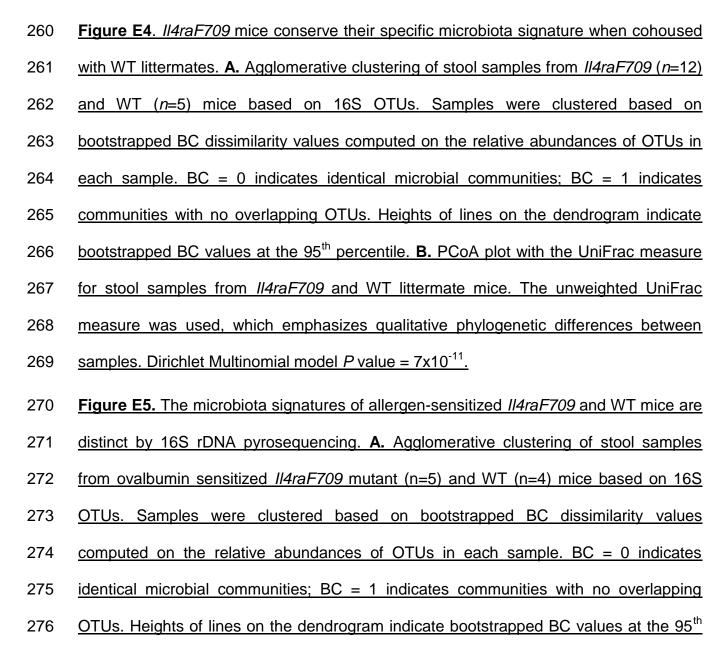
at the 95th percentile. **B.** Principal Coordinate Analysis (PCoA) plot with the UniFrac
 measure for stool samples from OVA and sham PBS sensitized *II4raF709* mice. The
 unweighted UniFrac measure was used, which emphasizes qualitative phylogenetic

239 differences between samples. *n*=5 for the *Il4raF709* OVA group versus 9 mice for the

240 <u>PBS sham sensitized *Il4raF709* group</u>. Dirichlet Multinomial model, *p*-value = $< 10^{-20}$.

241 Figure E2. T_R cell-treatment resets the microbiota of allergen-sensitized *II4raF709* mice 242 into a new baseline distinct from that of sham sensitized and treated control Il4raF709 243 mice. A. NMDS based on Weighted Unifrac distance between samples of PBS-244 sensitized mice (n=4) versus those of T_R-cell treated (n=5), OVA-sensitized mice, based 245 on the 786 taxa whose abundance was significantly different between groups using the 246 Kruskal-Wallis (KW) test. B. Hierarchical Clustering based on Weighted Unifrac 247 distance between samples. C. Nearest shrunken centroid analysis of OTUs that best 248 characterize the difference between allergen-sensitized versus tolerant groups. D. 249 Representation of the abundance of the OTUs identified by the nearest shrunken 250 centroid analysis using the PAM method.

Figure E3. The microbiota of sham-sensitized *Il4raF709* and WT mice are distinct. **A**. NMDS based on Weighted Unifrac distance between samples of PBS-sensitized *Il4raF709* mice (*n*=4) versus those of WT, PBS-sensitized mice (*n*=4), based on the 813 taxa whose abundance was significantly different between groups using the KW test. **B**. Hierarchical Clustering based on Weighted Unifrac distance between samples. **C**. Nearest shrunken centroid analysis of OTUs that best characterize the difference between allergen-sensitized versus tolerant groups. **D**. Representation of the abundance of the OTUs identified by the nearest shrunken centroid analysis using thePAM method.



277 percentile. B. PCoA plot with the UniFrac measure for stool samples from ovalbumin

278 sensitized mutant and WT mice. The unweighted UniFrac measure was used, which

279 emphasizes qualitative phylogenetic differences between samples. Dirichlet Multinomial

280 <u>model</u>, *p*-value = $< 10^{-20}$.

281 Figure E6. The microbiota signatures of allergen- (OVA +OVA/SEB) sensitized Il4raF709 and WT mice are distinct. A. NMDS based on Weighted Unifrac distance 282 283 between samples of OVA/SEB-sensitized WT (n=6) versus OVA+OVA/SEB sensitized 284 *Il4raF709* mice (*n*=9), based on the 430 taxa whose abundance was significantly 285 different between groups using the KW test. B. Hierarchical Clustering based on 286 Weighted Unifrac distance between samples. C. Nearest shrunken centroid analysis of 287 OTUs that best characterize the difference between the groups. D. Representation of 288 the abundance of the OTUs identified by the nearest shrunken centroid analysis using 289 the PAM method. E. Venn diagram showing the abundance levels of different OTUs in 290 relation to the sensitization state of WT and II4raF709 mice. The labels define the 291 abundance states of sets of OTUs in relation to specific comparison groups, e.g. F709 292 OVA+OVA/SEB<F709 PBS identifies those OTUs that are less abundant in allergen 293 sensitized (with OVA or with OVA/SEB) *II4raF709* mice as compared to sham (PBS) 294 sensitized mice. The number of OTUs thus identified is indicated in parentheses. 295 Spheres indicate intersections between two sets, while the colored webs show which 296 intersection of sets form the spheres. F. Contingency table representation of the results shown in the Venn diagram. P<0.0001 by the X² test (excluding the 2993 OTUs that did 297 298 not change upon sensitization in both WT and *II4raF709* mice).

Table E1. Annotations of Prediction Analysis for Microarrays (PAM)-selected bacterial
taxa that discriminate between sham and allergen (OVA and OVA/SEB-sensitized) *Il4raF709* mice (see Figure 3C, D).

Table E2. Annotations of bacterial taxa showing significantly different abundances between sham and allergen-sensitized *II4raF709* mice, as shown in the phylogenetic tree in **Figure 4**.

305 **Table E3.** Annotations of bacterial genera that optimally discriminate between sham

306 and allergen-sensitized Il4raF709 mice, as revealed by 16S rDNA pyrosequencing

307 (Figure E1) and determined using the Random Forest machine learning method.

308 **Table E4**. Annotations of PAM-selected bacterial taxa that discriminate between 309 allergen (OVA- and OVA/SEB)-sensitized versus T_R -cell treated and OVA-sensitized 310 mice. The taxa selected correspond to those graphically presented in **Figure 5C, D**.

311 **Table E5.** Annotations of bacterial taxa showing significantly different abundances 312 between sham and allergen-sensitized *II4raF709* mice, as shown in the phylogenetic 313 tree in **Figure 6**.

Table E6. Annotations of PAM-selected bacterial taxa that discriminate between T_R celltreated, allergen (OVA)- and sham-sensitized *II4raF709* mice. The taxa selected correspond to those graphically presented in **Figure E2C**, **D**.

Table E7. Annotations of PAM-selected bacterial taxa that discriminate between shamand allergen (OVA/SEB)-sensitized WT mice. The taxa selected correspond to those
graphically presented in Figure E3C, D.

320 **Table E8**. Annotations of PAM-selected bacterial taxa that discriminate between 321 allergen (OVA/SEB)-sensitized WT *and II4raF709* mice. The taxa selected correspond 322 to those graphically presented in **Figure 7C**, **D**.

323	<u>Table</u>	e E9. Annotations of bacterial genera that optimally discriminate between allergen-
324	<u>sensi</u>	tized WT versus Il4raF709 mice, as revealed by 16S rDNA pyrosequencing
325	<u>(Figu</u>	re E5) and determined using the Random Forest machine learning method.
326	Sup	plementary References
327	1.	Hazen TC, Dubinsky EA, DeSantis TZ, Andersen GL, Piceno YM, Singh N, et al.
328		Deep-sea oil plume enriches indigenous oil-degrading bacteria. Science 2010;
329		330:204-8.
330	2.	Lozupone C, Hamady M, Knight R. UniFracan online tool for comparing
331		microbial community diversity in a phylogenetic context. BMC Bioinformatics
332		2006; 7:371.
333	3.	Lozupone C, Knight R. UniFrac: a new phylogenetic method for comparing
334		microbial communities. Appl Environ Microbiol 2005; 71:8228-35.
335	4.	Legendre P, Legendre L. Numerical ecology. 2nd English ed. Amsterdam ; New
336		York: Elsevier; 1998.
337	5.	Shepard RN. Multidimensional scaling, tree-fitting, and clustering. Science 1980;
338		210:390-8.
339	6.	Tibshirani R, Hastie T, Narasimhan B, Chu G. Diagnosis of multiple cancer types
340		by shrunken centroids of gene expression. Proc Natl Acad Sci U S A 2002;
341		99:6567-72.
342	7.	Price MN, Dehal PS, Arkin AP. FastTree 2approximately maximum-likelihood
343		trees for large alignments. PLoS One 2010; 5:e9490.

- DeSantis TZ, Hugenholtz P, Larsen N, Rojas M, Brodie EL, Keller K, et al.
 Greengenes, a chimera-checked 16S rRNA gene database and workbench
 compatible with ARB. Appl Environ Microbiol 2006; 72:5069-72.
- 347 9. Letunic I, Bork P. Interactive Tree Of Life (iTOL): an online tool for phylogenetic
 348 tree display and annotation. Bioinformatics 2007; 23:127-8.
- Mosimann JE. On the compound multinomial distribution, the multivariate β distribution, and correlations among proportions. Biometrika 1962; 49:65-82.
- 351 11. Tvedebrink T. Overdispersion in allelic counts and theta-correction in forensic
 352 genetics. Theor Popul Biol 2010; 78:200-10.
- Bray JR, Curtis JT. An Ordination of the Upland Forest Communities of Southern
 Wisconsin. Ecological Monographs 1957; 27:325-49.
- 355 13. Breiman L. Random Forests. Learning Machines 2001; 45:5-32.
- 356 14. Kursa MB, Rudnicki WR. Feature selection with the boruta package. j. Stat. Soft.
 357 2010; 36:1-13.
- 358 15. Caporaso JG, Kuczynski J, Stombaugh J, Bittinger K, Bushman FD, Costello EK,
- et al. QIIME allows analysis of high-throughput community sequencing data. Nat
 Methods 2010; 7:335-6.
- 361 16. Schloss PD, Westcott SL, Ryabin T, Hall JR, Hartmann M, Hollister EB, et al.
 362 Introducing mothur: open-source, platform-independent, community-supported
 363 software for describing and comparing microbial communities. Appl Environ
 364 Microbiol 2009; 75:7537-41.

365	17.	Angiuoli SV, Matalka M, Gussman A, Galens K, Vangala M, Riley DR, et al.
366		CloVR: a virtual machine for automated and portable sequence analysis from the
367		desktop using cloud computing. BMC Bioinformatics 2011; 12:356.

368